# Calculation of optical transport and localization quantities

E. N. Economou
*Research Center of Crete and Department of Physics,* P.O. Box 1527, 711 10 Iraklio, Crete, Greece;*
*Corporate Research Science Laboratory, Exxon Research and Engineering Company, Annandale, New Jersey 08801;*
*and Ames Laboratory, U.S. Department of Energy, Iowa State University, Ames, Iowa 50011*

C. M. Soukoulis
*Ames Laboratory, U.S. Department of Energy and Department of Physics,* Iowa State University, Ames, Iowa 50011*
*and Corporate Research Science Laboratory, Exxon Research and Engineering Company, Annandale, New Jersey 08801*
(Received 20 March 1989)

By combining a coherent-potential approximation with our previous work on localization, we calculate the mean free path $l$, the diffusion coefficient $D$, the localization parameter $kl$, where $\mathbf{k}$ is the renormalized wave vector, the localization length $L_c$, and other related quantities. Our results for $D$ near the critical regime are in surprisingly impressive agreement with recent experimental data by Drake and Genack in a sample of titania spheres in air. Our calculations indicate that optical localization can be experimentally realized by either lowering the concentration of the titania spheres or lowering the standard deviation of the radii distribution.

The question of optical or, more generally, classical wave localization (CWL) has been examined[1,2] both experimentally[3-8] and theoretically.[9-11] Until recently, there was no conclusive evidence supporting the proposal that CWL is indeed possible in disordered systems characterized by a positive-definite random dielectric function. Recently, Soukoulis *et al.*[12] studied the question of CWL in a lattice model by employing a reliable numerical technique; they found that localization does indeed take place in their model, and they argued that CWL is more easily attainable in a realistic system of spheres of dielectric constant $\epsilon_2>0$ randomly embedded in a host material of dielectric function $\epsilon_1(0<\epsilon_1<\epsilon_2)$ rather than in their discrete numerical tight-binding model. In the same work,[12] a coherent-potential approximation (CPA) was developed which is equally applicable to scalar or vector wave equations and which is almost free from spurious multiple solutions and other related misbehaviors quite common when simple CPA is applied to continuum models. This CPA combined with the potential-well-analogy (PWA) approach[13] to the localization problem yields results consistent with the numerical data in the regime where the latter are relevant, i.e., for not so high $\omega$ and $x$ ($\omega$ is the frequency and $x$ is the volume fraction occupied by the spheres).

In a recent paper Drake and Genack[14] reported measurements of the optical diffusion coefficient $D$ and absorption time in a sample of closed-packed titania spheres $[(\epsilon_2)^{1/2}=2.2]$ of average radius $\bar{a}=3000$ Å in air $[(\epsilon_1)^{1/2}=1]$. They found values of $D$ as low as $1.45\times10^4$ $\mathrm{cm}^2/\mathrm{sec}$ showing clearly that the critical regime very close to localization has been reached for the first time.

In this Brief Report, we report theoretical results based on our simple CPA (Ref. 12) and the PWA (Ref. 13) for values of the parameters pertinent to the Drake and Genack experiment.[14] Our simple CPA replaces the randomly varying dielectric function $\epsilon(\mathbf{r})$ [$\epsilon(\mathbf{r})=\epsilon_2$ for $\mathbf{r}$ inside a titania sphere and $\epsilon_1=1$ outside] by an effective, complex, uniform $\epsilon_e$ from which an effective propagation constant $q\equiv(\epsilon_e)^{1/2}\omega/c$ is defined, where $c$ is the velocity of light. The quantity $\epsilon_e$ is determined by the condition $\langle C\rangle=0$, where $\mathrm{Im}C$ is the total cross section (TCS) times $\mathrm{Re}q/4\pi$. This TCS is associated with the scattering induced by the replacement of $\epsilon_e$ within a sphere by either $\epsilon_2$ or $\epsilon_1$. The average is over these two possibilities and over the distribution of sphere radii, if any. The TCS is defined as the total normalized flux of the outgoing spherical wave just outside the sphere plus the normalized absorption (if any) within the sphere minus the normalized "absorption" of the incident wave of propagation constant $q$ within a sphere of equal size.[15] The CPA equation $\langle C\rangle=0$ was brought to the form $q_{n+1}=q_n+A\langle C\rangle$, where $q_n=[(E-\Sigma_n)2m/\hbar^2]^{1/2}$, $\Sigma$ is the self-energy, $n$ is the order of iteration, and $A$ is chosen using the weak scattering limit and demanding as good a convergence as possible. We used $A=3/2q_n$ and the CPA equation was solved numerically by iteration, which in almost all cases converged to a unique solution. Once $q$ has been determined, one can find immediately the mean free path $l=0.5/\mathrm{Im}q$, the renormalized wave vector $k=\mathrm{Re}q$, the dimensionless localization parameter $kl$, the effective phase velocity $v=\omega/k$, and the Boltzmann diffusion coefficient $D_0=\frac{1}{3}vl$. In this formula, $l$ is supposed to be the transport mean free path, $l_{\mathrm{tr}}$, which is defined as the length over which momentum transfer becomes uncorrelated. This is different from scattering mean free path which describes the decay length of the single-particle Green's function. The two mean free paths are related by $l_{\mathrm{tr}}=(1-\cos\theta)l$ in the most simple circumstances. Here we have used that $l_{\mathrm{tr}}=l$, which is certainly not true for the $p$-spherical harmonic Mie resonance. Using these CPA results, one can obtain various localization quantities on either side of the critical point by employing the

 

PWA expressions.[13] These simple approximation expressions have been checked successfully up to now against various numerical data. According to the PWA the critical point, i.e., the so-called mobility edge, where localization just sets in, is given by[13]

$$(kl)_c = 0.844 \ . \tag{1}$$

It is convenient to define $\phi \equiv (kl)^2/(0.844)^2$. We have then for $\phi > 1$ (i.e., on the extended side)[13]

$$D = D_0 f^{-1} \ , \tag{2}$$

where $f = 1 + 6/\phi(\phi - 1)$, $D$ is the diffusion coefficient, and $f^{-1}$ is its reduction factor due to amplitude fluctuations which eventually may lead to localization. Besides $D$, another quantity that can be measured directly experimentally is the quasi-one-dimensional localization length $L_A$ in a wire of cross section $A$ made from our composite material and surrounded by a perfectly reflecting wall:

$$L_A = \frac{A}{4.82\xi} \ , \tag{3}$$

where $\xi$, the correlation length, is given by $\xi = 2.72lf/\phi$. On the localized side ($\phi < 1$) the localization length $L_c$ is given by[13]

$$L_c = l(2.2 + 14.12\phi)/(1 - \phi) \ .$$

In Fig. 1, we plot our result for $D$, $kl$, $l$, and $L_A/A$ versus $\lambda_1/\bar{a}$ ($\lambda_1 = \lambda_0/\sqrt{\epsilon_1}$ where $\lambda_0$ is the wavelength in vacuum) together with the experimental data from Ref. 14. All the parameters in our calculations are fixed by the experimental conditions ($\epsilon_1 = 1$, $\epsilon_2 = 4.84$, $\bar{a} = 3000$ Å, $\sigma_a/\bar{a} = 0.29$, where $\sigma_a$ is the standard deviation of the radii distribution assumed rectangular[16]). The only parameter which is not known accurately is the sphere volume fraction $x$. Due to the way the sample was prepared, it is reasonable to assume that we have random close packing. For spheres of equal size, random close packing corresponds[17] to $x = 63.7\%$. In the present case where there is large variation ($\sigma_a/\bar{a} = 0.29$), we expect that $x$ will be appreciably larger than 63.7%. We found that the results depend rather sensitively on $x$ (for $x$ in the range 50–75 %) and that $x = 73\%$ fits the experimental data well, as can be seen from Fig. 1. Such an agreement is really impressive given the absence of free parameters in our theory and the simplicity of our CPA. In this connection, it is worthwhile to point out that one would expect that our CPA would given an optimum $x$ for localization, $x_{\text{opt}}$, lower than 0.50. The reasons are that (i) our CPA treats the $A$ and $B$ components completely equivalently, and (ii) a $B$ sphere in an $A$ host is a more efficient scatterer than an $A$ sphere in a $B$ host. On the other hand, preliminary results[18] for a periodic arrangement of spheres show that scalar waves are subject to strong multiscattering processes near the position of the second $l = 2$ and the third $l = 1$ Mie resonances even for as high an $x$ as 0.74.

It is rather surprising that the single-sphere Mie resonant scattering is the dominant scattering factor in concentrations as high as 0.74. A possible explanation[18] for this dominant role of the single sphere may be associated with its spherical symmetry. Indeed, the spherical scatterers as opposed, e.g., to the cubic scatterers cannot form new well-connected shapes by clustering together. Thus, new cluster resonances cannot easily appear. This geometric effect is also related to the fact that nonoverlapping spheres cannot form percolating channels even in the closed-packed limit of $x \simeq 0.74$, while for other geometries a percolation channel opens up for $x = 0.15$. It is, therefore, the persistence of the dominant role of the single scatterer, even for high $x$, that makes the CPA ap-

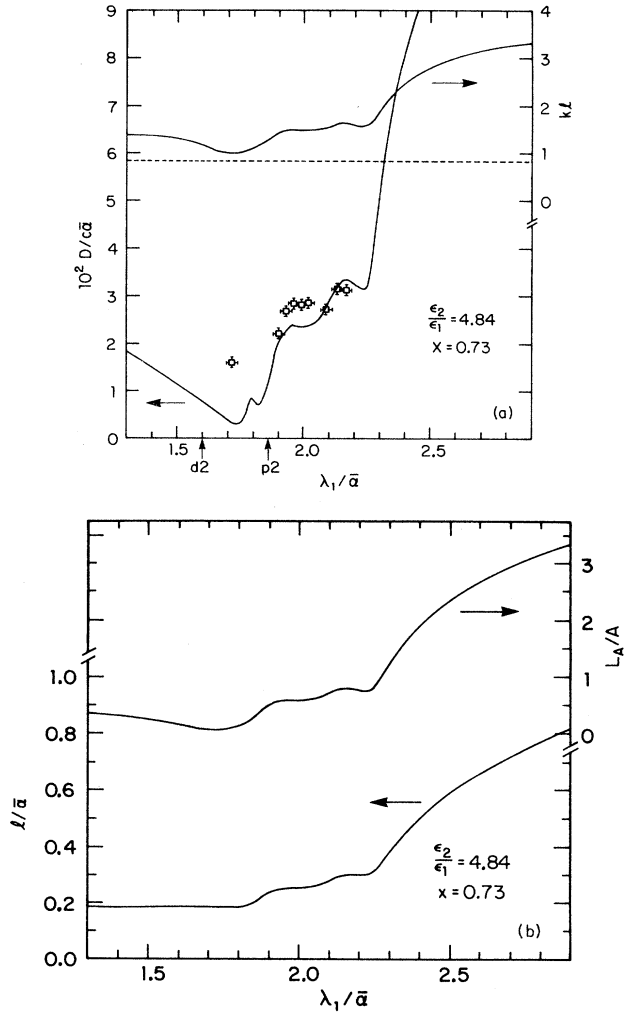


FIG. 1. (a) Diffusion constant ($10^2 D/c\bar{a}$, where $c$ is the velocity of light) and the localization parameter $kl$, (b) mean free path $l/\bar{a}$ and $L_A/A$ as a function of the wavelength $\lambda_1/\bar{a}$, for a sample of tinania spheres ($\epsilon_2 = 4.84$) in air ($\epsilon_1 = 1$). The concentration of spheres is $x = 0.73$, while the standard deviation of the sphere radii distribution is $\sigma_a/\bar{a} = 0.29$, where $\bar{a}$ is the average radius of the spheres. The squares with error bars represent the measured experimental data of Drake and Genaek for the same set of parameters. The dashed line represents the value $kl \simeq 0.844$, which is the critical value of localization. The arrows $d_2$ and $p_2$ on the $\lambda_1/\bar{a}$ axis represent the positions of the second resonances of the $l = 2$ and $l = 1$ components, respectively.

proach reliable. Thus, in the absence of a direct calculational test of the CPA at such high volume fractions $x$, it is not clear whether the CPA tends to overestimate $x_{opt}$ or, more generally, whether the CPA results are as accurate as their agreement with the experimental data is suggesting. At the point $\lambda_1/\bar{a} \simeq 1.71$, the value of $kl$ is 1, i.e., very close to the critical value (0.844) for localization; the mean free path is $l = 0.19 \times 3000$ Å $= 570$ Å, close to the estimate given in Ref. 14; the reduction factor is $f^{-1} = 0.176$; and the renormalized phase velocity is $1.84 \times 10^8$ m/sec $= 0.615c$, where $c$ is the velocity of light. The localization that was almost observed at $\lambda_1/\bar{a} \simeq 1.7$ is due to the combined effect of the second resonances of the $l = 1$ and $l = 2$ components. The positions of these resonances, denoted by $p2$ and $d2$, respectively, are shown in Fig. 1. As can be seen from Fig. 1, we have specific predictions for the quasi-one-dimensional localization length $L_A$ as a function of the wavelength $\lambda_1/\bar{a}$. These predictions can be tested experimentally.

In Fig. 2, we plot our calculated values for $D$ and $kl$ for the same parameters as before except $x$, which is now taken to be 60%. We see that the second resonances, $p2$ and $d2$, are not now as effective as they were for higher $x$ (the minimum at $\lambda_1/\bar{a} \simeq 1.7$ disappeared), while the lowest (i.e., the first) resonances of $l = 1$ and $l = 2$ character (denoted by $p1$ and $d1$, respectively) now produce strong effects. Indeed the $p1$ is responsible for the true localization for $3 \leq \lambda_1/\bar{a} \leq 3.6$ and the $d1$ for the local minimum at $\lambda_1/\bar{a} = 2.4$. The minimum value of the localization length is obtained at $\lambda_1/\bar{a} \simeq 3.45$ and is equal to $6.6\bar{a}$; the corresponding values of $l$ and $v$ are $0.3\bar{a}$ and $0.89c$; respectively. The results shown in Fig. 2 are important because they suggest that true localization can be observed in a system of polydisperse titania spheres in air. What is needed is to lower the volume fraction of the titania spheres (this can be achieved by diluting them with spheres of dielectric constant equal to 1) and choose their average radius and the wavelength so that $\lambda_1/\bar{a} = 3 \pm 0.5$. Our calculations also show that it is possible to obtain localization for a given concentration $x$ by decreasing the width of the distribution of the sphere radii. As $\sigma_a$ decreases, we observe strong variations of $D$, $kl$, and other transport quantities as a function of the wavelength. In particular, for $x = 0.60$ and $\sigma_n/\bar{a} = 0.05$, we obtain localization not only at $\lambda_1/\bar{a} \simeq 3.0$, but also around $\lambda_1/\bar{a} \simeq 2.0$, which is close to the $p2$ resonance. The same is true for $x = 0.73$ and $\sigma_a/\bar{a} = 0.05$, where we obtain localization at $\lambda_1/\bar{a} = 2.3$, which is close to the $d1$ resonance, as well as at $\lambda_1/\bar{a} = 1.5$, which is due to the $d2$ resonance.

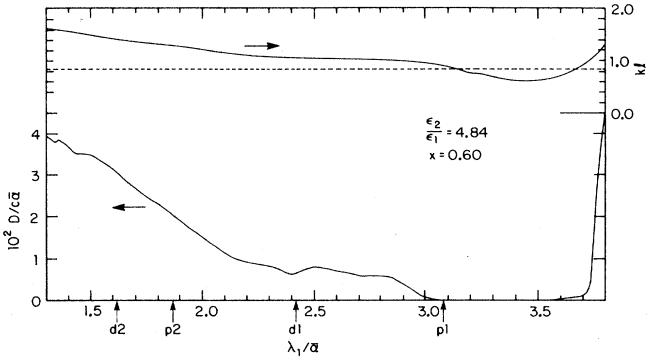


FIG. 2. Diffusion constant ($10^2 D/c\bar{a}$) and the localization parameter $kl$ as a function of the wavelength $\lambda_1/\bar{a}$ for a sample of tinania spheres ($\epsilon_2 = 4.84$) in air ($\epsilon_1 = 1$). All the parameters are exactly as those in Fig. 1 except that $x = 0.60$. The arrows $d_2$, $p_2$, $d_1$, and $p_1$ in the $\lambda_1/\bar{a}$ axis represent the positions of the second and first resonances of the $l = 2$ and $l = 1$ components, respectively.

In conclusion, we have calculated, through a well-converged CPA, different transport quantities for electromagnetic waves, such that $D$, $l$, $kl$, $L_c$, and $L_A/A$ agree very well with the experiment of Drake and Genack. This is so, provided that the one free parameter of our theory, the concentration $x$ of the titania spheres, is 73%. Our theory predicts that true localizations can be achieved with a sample of titania spheres in air provided that either the sphere concentration $x$ is lowered by about 15% or the standard deviation of the radii distribution $\sigma_a/\bar{a}$ is lowered to about 5%. Although the impressive agreement of our CPA results with the experimental data makes our method a serious candidate for obtaining reliable quantitative results, it will nevertheless, be very interesting to check the CPA results for the EM case against more reliable numerical techniques, as has been done for the scalar wave equation.[12]

We thank A. Genack for several helpful discussions and for giving us the experimental results before publication. This work was partially supported by North Atlantic Treaty Organization Grant No. RG769/87. Ames Laboratory is operated for the U. S. Department of Energy by Iowa State University under Grant No. W-7405-ENG-82. This investigation was supported by the Director for Energy Research, Office of Basic Energy Sciences.

*Permanent address.

[1]S. John, Phys. Rev. Lett. **53** 2169 (1983); Phys. Rev. B **32**, 304 (1985); Comments Condensed Matter Phys. **14**, 193 (1988).
[2]P. W. Anderson, Philos. Mag. B **52**, 505 (1985).
[3]Y. Kugu and A. Ishimaru, J. Opt. Soc. Am. A **1**, 831 (1984).
[4]M. P. Van Albada and A. Lagendijk, Phys. Rev. Lett. **55**, 2692 (1985).
[5]P. E. Wolf and G. Maret, Phys. Rev. Lett. **55**, 2696 (1985).
[6]S. Etemad, R. Thomson, and M. J. Andrejco, Phys. Rev. Lett. **57**, 575 (1986).

[7]A. Z. Genack, Phys. Rev. Lett. **58**, 2043 (1987).
[8]M. Kaveh, M. Rosenbluh, I. Edrei, and I. Freund, Phys. Rev. Lett. **57**, 2049 (1986).
[9]Ping Sheng and Z. Q. Zhang, Phys. Rev. Lett. **57**, 1879 (1986).
[10]K. Arya, Z. B. Su, and J. L. Birman, Phys. Rev. Lett. **57**, 2725 (1986).
[11]C. A. Condat and T. R. Kirkpatrick, Phys. Rev. Lett. **58**, 226 (1987).
[12]C. M. Soukoulis, E. N. Economou, G. S. Grest, and M. H. Cohen, Phys. Rev. Lett. **62**, 575 (1989).
[13]E. N Economou, C. M. Soukoulis, and A. D. Zdetsis, Phys. Rev. B **30**, 1686 (1984); **31**, 6483 (1985); E. N. Economou, C. M. Soukoulis, M. H. Cohen, and A. D. Zdetsis, *ibid.* **31**, 6172 (1985); E. N. Economou, *ibid.* **31**, 7710 (1985).
[14]J. M. Drake and A. Z. Genack, Phys. Rev. Lett. **63**, 259 (1989).
[15]The TCS for the electromagnetic case as defined in this work is given by $4\pi\,\mathrm{Im}C/\mathrm{Re}q$, where

$$C=(qa^2/2)\sum_{l=1}^{\infty}(2l+1)[j_l^* h_l'(r_l+\bar{r}_l)+j_l' h_l^*(r_l^*+\bar{r}_l^*)]\ ,$$

$a$ is the radius of the sphere, $j_l$ is the spherical Bessel function, $h_l$ is the spherical Hankel function of the first kind, an asterisk indicates complex conjugate, a prime denotes differentiation with respect to the argument which is $qa$, and $r_l,\bar{r}_l$ are as given in Ref. 12. For real $q$, we have that

$$C=\frac{i}{2q}\sum_{l=1}^{\infty}(2l+1)(r_l+\bar{r}_l)=f(0)\ ,$$

where $f(0)$ is the forward scattering amplitude.
[16]We have also used a Gaussian distribution for the radii with slightly different results.
[17]R. Zallen, *Physics of Amorphous Solids* (Wiley, New York, 1983).
[18]E. N. Economou and A. D. Zdetsis, Phys. Rev. B **40**, 1334 (1989).